第 43 卷 第 14 期/2023 年 7 月/光学学报

研究论文

光学学报

基于共振腔发光二极管的DBR温度特性研究

任凯兵，李建军*，崔屿峥，张振东，付聪乐，邓军

北京工业大学光电子技术教育部重点实验室，北京 100124

摘要 分布式布拉格反射镜(DBR)是共振腔发光二极管(RCLED)的主要组成部分，其温度特性对RCLED的性能有着重要影响。基于650 nm红光RCLED，设计出由$Al_{0.5}Ga_{0.5}As$和$Al_{0.95}Ga_{0.05}As$组成的DBR结构。首先通过$Al_xGa_{1-x}As$材料折射率的色散关系分析温度对$Al_xGa_{1-x}As$材料折射率的影响，进而模拟了DBR反射谱的温度特性，得到随着温度升高DBR反射谱红移的结论，温漂速率为0.048982 nm/℃。通过MOCVD制备出30对$Al_{0.5}Ga_{0.5}As$和$Al_{0.95}Ga_{0.05}As$组成的DBR外延结构，并对其进行反射谱测试，发现随着温度升高反射谱出现了红移现象，温漂速率为0.049277 nm/℃，与模拟结果相近，验证了温度升高导致反射谱红移结论的正确性。

关键词 共振腔发光二极管；分布式布拉格反射镜；温度；色散关系；外延

中图分类号 TN29 **文献标志码** A **DOI:** 10.3788/AOS230623

1 引言

共振腔发光二极管(RCLED)是指将发光有源区置于共振腔内的发光二极管[1]。RCLED具有高亮度、高效率，以及更好的方向性、更纯的光谱纯度，其应用范围越来越广泛，特别是出射波长为650 nm的红光RCLED以其优异的特性在塑料光纤通信领域、显示照明领域都有良好的应用前景[2]。相比于普通发光二极管[3-4]，RCLED由于微腔效应使有源区的自发辐射光在腔中形成共振，从而提高出射光的光谱纯度，改善了出光方向，大大提高了外量子效率。相比于垂直腔面发射激光器(VCSEL)，虽然二者有着相似的结构，但是RCLED的工艺制备较为简单，成本更低，并且RCLED没有VCSEL的阈值电流限制，所需驱动电流小[5]。

RCLED的基本结构主要由上、下分布式布拉格反射镜(DBR)和夹在反射镜之间的有源区三部分组成，其中具有可调节反射率的DBR在LED、激光器等光电器件中具有广泛的应用[6]，DBR的特性对包括RCLED在内的光电器件的性能有着重要影响。出射波长为650 nm的红光RCLED用于塑料光纤通信时要与光纤耦合，耦合效率与RCLED出射光的远场分布有关，共振腔膜与量子阱的发射光波长的失谐程度会随着温度变化而改变进而影响RCLED出射光的远场分布[7]。谐振腔膜的变化主要与DBR反射谱的温度漂移有关，从而导致反射中心波长移动。研究表明，谐振腔膜与量子阱增益峰值波长的温漂速度不同，在非室温时可能导致二者失配，从而影响器件的出光性能[8]。本文基于650 nm的红光RCLED的DBR外延结构，模拟分析了温度变化对DBR的影响，并且通过实验制备了红光RCLED的DBR外延结构，与模拟结果进行对比分析，验证了DBR随温度的变化关系。相关结果对温度敏感性更高的VCSEL的设计也具有一定参考与指导意义。

2 DBR的温度特性模拟

2.1 DBR材料的选择

DBR是由光学厚度为1/4出射波长的两种不同折射率的半导体或介质材料交替生长构成的。目前红光RCLED的有源区一般采取基于AlGaInP的材料系，衬底一般选取GaAs材料，DBR材料系一般可选为AlGaInP和$Al_xGa_{1-x}As$材料系。由于$Al_xGa_{1-x}As$材料系与GaAs衬底的晶格更为匹配，所以DBR的材料选择使用$Al_xGa_{1-x}As$材料系。DBR的反射率与两种材料的折射率差和DBR对数有关，DBR的反射率计算公式[9]为

$$R=\left[\frac{n_0-\dfrac{n_H^2}{n_S}\left(\dfrac{n_H}{n_L}\right)^{2m}}{n_0+\dfrac{n_H^2}{n_S}\left(\dfrac{n_H}{n_L}\right)^{2m}}\right]^2, \tag{1}$$

式中：n_0为入射介质的折射率；n_H为高折射率材料的折

收稿日期：2023-03-02；**修回日期**：2023-03-21；**录用日期**：2023-04-03；**网络首发日期**：2023-04-13

基金项目：国家重点研发计划(2018YFA0209003)、北京市自然科学基金(4222060)

通信作者：*lijianjun@bjut.edu.cn

射率；n_L为低折射率材料的折射率；n_S为衬底的折射率；m为DBR的对数。可以看出，DBR的反射率大小和两种材料的折射率差以及DBR对数呈正相关关系。

$Al_xGa_{1-x}As$材料系的折射率与Al组分相关，根据有关文献报道[10]，$Al_xGa_{1-x}As$的折射率大小和Al组分高低呈负相关关系，因此需要选择高、低Al组分的$Al_xGa_{1-x}As$作为生长DBR结构的低、高折射率材料。对于高折射率的低Al组分材料，GaAs是理论上折射率最高的选择，但是考虑到GaAs材料对红光有很强的吸收性，所以GaAs一般用于红外波段的发光器件中。对于$Al_xGa_{1-x}As$材料来说，对红光的吸收与其禁带宽度有关，室温下其禁带宽度与Al组分的关系[11]为

$$E_g(x)=\begin{cases}1.424+1.24x, x\leqslant 0.45\\ 1.9+0.125x+0.143x^2, x>0.45\end{cases}。\tag{2}$$

由式(2)可得，$Al_xGa_{1-x}As$材料在Al组分小于0.45时是直接带隙材料，在Al组分大于0.45时，$Al_xGa_{1-x}As$成为间接带隙材料。禁带宽度与辐射波长的关系可以通过$E_g(\mathrm{eV})=1.24/\lambda(\mu\mathrm{m})$表达式确定。由于出射波长为650 nm，对应的禁带宽度为1.908 eV，因此为了减少DBR对有源区发出的光的吸收，$Al_xGa_{1-x}As$的禁带宽度应当大于1.908 eV，如图1所示。因此选择$Al_xGa_{1-x}As$材料的Al组分应当使$E_g>$0.388 eV。又因为直接带隙材料相比间接带隙材料对光的吸收更强，因此为了减少DBR对光的吸收，DBR材料选择间接带隙材料。综上，本文选择$Al_{0.5}Ga_{0.5}As$作为DBR的低Al组分材料。

对于低折射率的高Al铝的组分材料，AlAs是理论上的最好选择，但是要考虑器件氧化带来的问题。$Al_xGa_{1-x}As$材料在器件中氧化产生的氧化物是$(Al_xGa_{1-x})O_3$的非晶固溶体，氧化物层的厚度在达到一定温度后会有所减少，有实验测量出Al组分越高的$Al_xGa_{1-x}As$形成的氧化物层的厚度收缩率越高，而氧化层厚度的减少会导致氧化层末端产生应变场[12]。因此，本文不选择使用Al组分较高的AlAs和$Al_{0.98}Ga_{0.02}As$材料，而选择$Al_{0.95}Ga_{0.05}As$作为DBR的高Al组分材料。

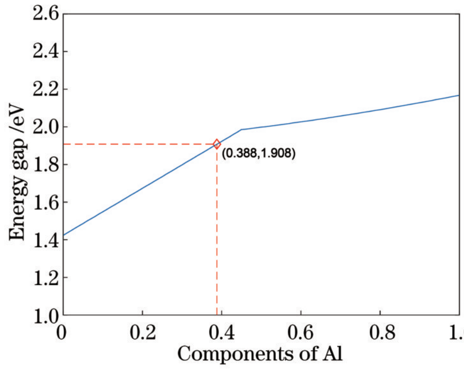

图1　$Al_xGa_{1-x}As$的禁带宽度与Al组分的关系

Fig. 1　Relationship between the gap width of $Al_xGa_{1-x}As$ and the components of Al

2.2　$Al_xGa_{1-x}As$材料折射率的色散关系

DBR的温度特性主要和$Al_xGa_{1-x}As$材料的折射率的色散关系相关[10]，$Al_xGa_{1-x}As$的折射率与Al组分x、温度T和入射波长λ有关。文献[10]给出了$Al_xGa_{1-x}As$的折射率与x、T和λ三个变量的拟合函数，

$$n^2(x)=A(x)+\frac{C_0(x)}{E_0^2(x)-E^2}+\frac{C_1(x)}{E_1^2(x)-E^2}+R(x),\tag{3}$$

式中：$R(x)$是修正项，受三元化合物影响很小，可忽略不计；$E=\frac{hc}{\lambda}$是光子能量。$A(x)$、$1/C_0(x)$、$E_0(x)$、$C_1(x)$、$E_1^2(x)$都具有以下形式，

$$c(x,T)=c_0(T)+c_1\cdot x+c_2\cdot x^2+c_3\cdot x^3+c_4\cdot x^4+c_5\cdot x^5。\tag{4}$$

表1中给出了以上公式具体的参数，表中$A_0(T)$和$E_{10}^2(T)$是关于温度的二阶多项式，可由如下表达式给出，

$$A_0(T)=a_0+a_1\cdot T+a_2\cdot T^2,\tag{5}$$

$$E_{10}^2(T)=e_0+e_1\cdot T+e_2\cdot T^2,\tag{6}$$

式中各参数由表2给出。表2中$E_{\Gamma\mathrm{GaAs}}(T)$的表达式为

$$E_{\Gamma\mathrm{GaAs}}(T)=E_\Gamma(0)+S\cdot E_{\mathrm{Deb}}\left[1-\coth\left(E_{\mathrm{Deb}}/2k_BT\right)\right]+S_{\mathrm{TO}}\cdot E_{\mathrm{TO}}\left[1-\coth\left(E_{\mathrm{Deb}}/2k_BT\right)\right],\tag{7}$$

式中：$E_{\mathrm{Deb}}=1.59$ meV；$E_{\mathrm{TO}}=33.6$ meV；$S=1.8$；$S_{\mathrm{TO}}=1.1$；$k_B=0.0861708$ meV/K；$E_\Gamma(0)$是与材料有关的常数，在这里$E_\Gamma(0)=1.1592$ eV。

根据以上关于$Al_xGa_{1-x}As$折射率的拟合函数，分别计算了$Al_{0.5}Ga_{0.5}As$和$Al_{0.95}Ga_{0.05}As$的折射率与入射

表1　计算折射率n使用的参数

Table 1　Parameters used for calculating refractive index n

$c(x,T)$	A	$1/C_0/\mu m^2$	$C_1/\mu m^2$	$E_0/\mu m$	$E_1^2/\mu m^2$
c_0	$A_0(T)$	50.5350	21.5647	$E_{\Gamma\mathrm{GaAs}}(T)$	$E_{10}^2(T)$
c_1	−16.1590	−150.7000	113.7400	1.1308	11.0060
c_2	43.5110	−62.2090	−112.5000	0.1436	−3.0800
c_3	−71.3170	797.1600	108.4010	0	0
c_4	57.5350	−1125.0000	−47.3180	0	0
c_5	−17.4510	503.7900	0	0	0

表 2 计算 $A_0(T)$ 和 $E_{10}^2(T)$ 使用的参数

Table 2 Parameters used for calculating $A_0(T)$ and $E_{10}^2(T)$

$A_0(T)$	a_0	a_1 /K	a_2 /K^2
	5.9613	7.1780×10^{-4}	-0.9530×10^{-6}
$E_{10}^2(T)$	e_0	e_1 /K	e_2 /K^2
	4.7171	-3.2370×10^{-4}	-1.3580×10^{-6}

波长 λ 和温度 T 之间的关系，如图 2 所示。并且分别突出了当入射波长为 650 nm 时，$Al_{0.5}Ga_{0.5}As$ 和 $Al_{0.95}Ga_{0.05}As$ 的折射率随温度的变化关系，以及当温度为 293.15 K 时折射率和入射波长的变化关系。可以看出：当波长不变时，二者的折射率随温度升高都小幅度增加；当在同一温度下时，二者的折射率随入射波长增加而减小。

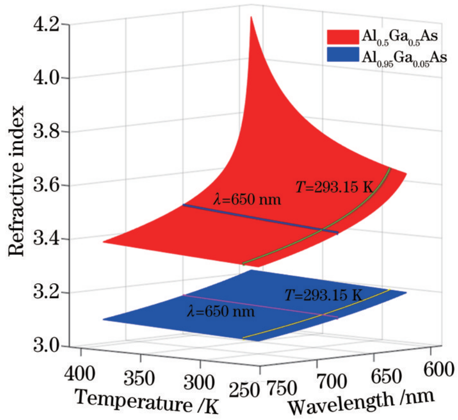

图 2 $Al_{0.5}Ga_{0.5}As$ 和 $Al_{0.95}Ga_{0.05}As$ 的折射率与入射波长和温度的关系

Fig. 2 Dependence of the refractive index of $Al_{0.5}Ga_{0.5}As$ and $Al_{0.95}Ga_{0.05}As$ on the incident wavelength and temperature

2.3 DBR 结构设计

根据式(3)，在 293.15 K 下且入射波长为 650 nm 时，$Al_{0.5}Ga_{0.5}As$ 和 $Al_{0.95}Ga_{0.05}As$ 的折射率分别为 3.4386 和 3.1215，根据 DBR 每层的物理厚度，可确定室温下用于 DBR 的 $Al_{0.5}Ga_{0.5}As$ 和 $Al_{0.95}Ga_{0.05}As$ 的厚度分别为 47.258 nm 和 52.059 nm。

根据薄膜的传输矩阵理论[13]，对三组不同的 $Al_xGa_{1-x}As$ 材料组合构成的 DBR 进行模拟计算，得到 DBR 反射率与对数的关系，如图 3 所示，可以看出，在 DBR 对数达到 30 对以上后，DBR 的反射率都能达到 90% 以上。虽然 DBR 对数增加可以提高反射率，但是会引起串联电阻增大导致器件发热增加从而影响器件性能，因此 DBR 的对数不能太高，本文选择对数为 30 对。

2.4 DBR 温度特性

根据薄膜传输矩阵理论，模拟了 293.15～393.15 K 不同温度下 30 对 $Al_{0.5}Ga_{0.5}As$ 和 $Al_{0.95}Ga_{0.05}As$ 组成的 DBR 反射谱，如图 4 所示。从模拟结果可以看出，随着温度的增加，DBR 的中心反射波长呈现向长波长方向移动的红移现象。温度对 DBR 反射谱的影响主要是通过影响 $Al_xGa_{1-x}As$ 的折射率，进而影响 DBR 材料的光学厚度从而改变反射谱。图 5 是中心波长随温度变化的线性拟合曲线，模拟所得 DBR 的中心波长随温度的漂移速率为 0.048982 nm/℃。

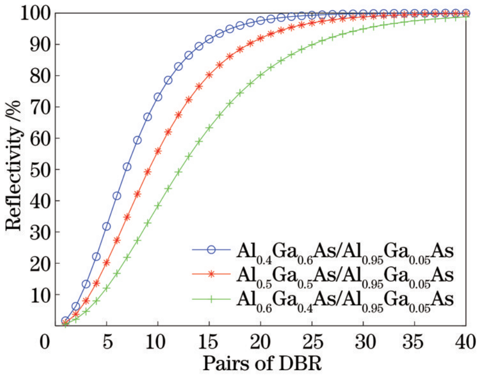

图 3 不同材料组合的 DBR 的反射率与对数的关系

Fig. 3 Relationship of DBR reflectivity with the pairs of DBR for different material combinations

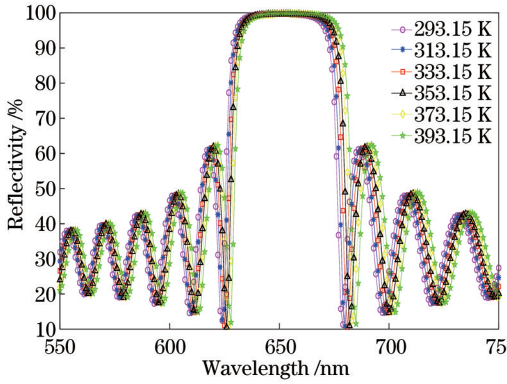

图 4 不同温度下 DBR 的反射谱

Fig. 4 Reflectance spectra of the DBR at different temperatures

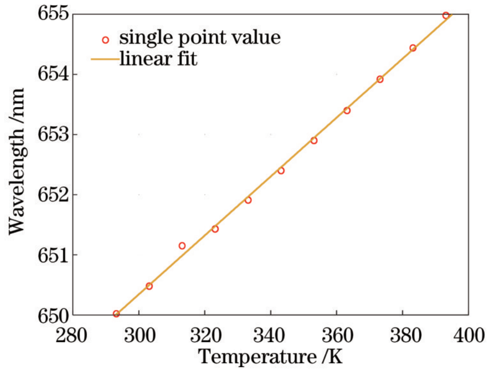

图 5 不同温度下 DBR 的中心反射波长

Fig. 5 Central reflection wavelength of the DBR at different temperatures

3 DBR 温度特性测试

3.1 DBR 结构制备

实验利用 MOCVD 外延技术，通过 EMCORE

D125 系统，在〈100〉偏〈111〉晶向的偏角 15°的 N 型 GaAs 衬底上，在 600 ℃的生长温度下进行外延材料生长。为了提高衬底与外延生长层的晶格匹配度，首先在衬底上生长 500 nm 厚的 GaAs 作为缓冲层，然后交替重复性生长 30 对 $\mathrm{Al_{0.5}Ga_{0.5}As}$ 和 $\mathrm{Al_{0.95}Ga_{0.05}As}$。生长过程中使用的载气是钯管纯化后的高纯 $\mathrm{H_2}$，使用 $\mathrm{AsH_3}$ 作为 As 源，MO 源以 TMAl 和 TMGa 分别作为 Al 源和 Ga 源。

3.2 DBR 测试

外延生长完成后，利用 Philip PLM-100 系统对外延片进行白光反射谱测试，测试过程中，通过 Linkam 公司的 T96 温控台在 20～120 ℃温度范围内控制外延片的温度，结果如图 6 所示。可见随着温度的升高反射谱确实出现了长波方向的红移。图 7 是其中心波长随温度的变化关系，实验测得中心波长随温度的漂移速率为 0.049277 nm/℃，这与模拟结果相近，验证了理论模拟结果的正确性。

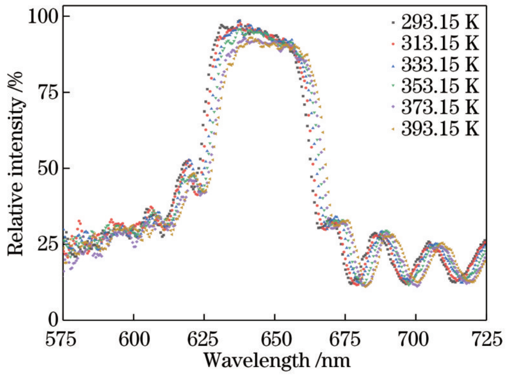

图 6　DBR 在不同温度下的白光反射谱

Fig. 6　White light reflection spectra of DBR at different temperatures

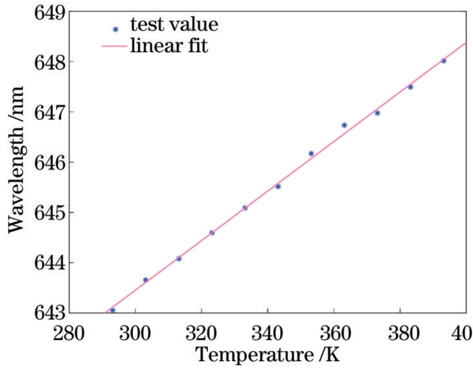

图 7　DBR 的中心波长随温度变化的关系

Fig. 7　Relationship between central wavelength of DBR and temperature variation

4　结　　论

本文基于出射波长为 650 nm 的红光 RCLED，设计了由 $\mathrm{Al_{0.5}Ga_{0.5}As}$ 和 $\mathrm{Al_{0.95}Ga_{0.05}As}$ 组成的 30 对 DBR 外延结构。由于 $\mathrm{Al_{x}Ga_{1-x}As}$ 折射率会随温度变化发生改变从而影响 DBR 的反射谱，理论分析了波长和温度对于 $\mathrm{Al_{0.5}Ga_{0.5}As}$ 和 $\mathrm{Al_{0.95}Ga_{0.05}As}$ 折射率的影响，模拟了其在不同温度下的反射谱，发现其随着温度升高向长波方向红移，并且得到理论的温漂系数为 0.048982 nm/℃。采用 MOCVD 进行了所设计的 DBR 的外延生长，并且对其进行白光反射谱测试，得到了反射谱随温度升高也红移的结果，测得的温漂系数为 0.049277 nm/℃，这与模拟结果相近，验证了理论的正确性。

通过测得的 DBR 反射谱的温漂系数，再结合量子阱出射波长与温度的变化关系，在室温下设计高温工作器件时要考虑量子阱和 DBR 等温漂系数的差异，实现高温下器件工作时量子阱、DBR 以及腔模之间波长的匹配，这个结论对于设计 VCSEL 这种对温度敏感性更高的器件也具有一定的指导意义。

参　考　文　献

[1] Schubert E F, Wang Y H, Cho A Y, et al. Resonant cavity light-emitting diode[J]. Applied Physics Letters, 1992, 60(8): 921-923.

[2] Moudakir T, Genty F, Kunzer M, et al. Design, fabrication, and characterization of near-milliwatt-power RCLEDs emitting at 390 nm[J]. IEEE Photonics Journal, 2013, 5(6): 8400709.

[3] 季渊，许怡晴，陈宝良，等．硅基微显示器发展现状与研究进展[J]. 激光与光电子学进展, 2022, 59(20): 2011007.
Ji Y, Xu Y Q, Chen B L, et al. Development status and research progress of silicon-based microdisplay[J]. Laser & Optoelectronics Progress, 2022, 59(20): 2011007.

[4] 马瑞青．RGB-LED 光源的峰值波长对其显色性的影响[J]. 激光与光电子学进展, 2021, 58(23): 2333002.
Ma R Q. Effect of peak wavelengths of RGB-LED light source on its color rendering property[J]. Laser & Optoelectronics Progress, 2021, 58(23): 2333002.

[5] 杨启伟，李建军．红光 RCLED 研究与进展[J]. 照明工程学报, 2021, 32(2): 36-43.
Yang Q W, Li J J. Research and development of red resonant cavity light-emitting diode[J]. China Illuminating Engineering Journal, 2021, 32(2): 36-43.

[6] 姚波，陈群峰，陈雨君，等．基于超稳腔 PDH 稳频的 280 mHz 线宽 DBR 光纤激光器[J]. 中国激光, 2021, 48(5): 0501014.
Yao B, Chen Q F, Chen Y J, et al. 280 mHz linewidth DBR fiber laser based on PDH frequency stabilization with ultrastable cavity[J]. Chinese Journal of Lasers, 2021, 48(5): 0501014.

[7] 马骏．多有源区共振腔发光二极管的结构设计与材料外延[D]. 北京：北京工业大学, 2010.
Ma J. Structural design and material epitaxy of multi-active region resonant cavity light-emitting diode[D]. Beijing: Beijing University of Technology, 2010.

[8] 张立森．大功率垂直腔面发射激光器的结构设计与研制[D]. 长春：中国科学院长春光学精密机械与物理研究所, 2012: 37-39.
Zhang L S. Structural design and development of high power vertical cavity surface emitting laser[D]. Changchun: Changchun Institute of Optics, Fine Mechanics and Physics, Chinese Academy of Sciences, 2012: 37-39.

[9] 张建伟，宁永强，张星，等．高温工作垂直腔面发射半导体激光器现状与未来(特邀)[J]. 光子学报, 2022, 51(2): 0251201.
Zhang J W, Ning Y Q, Zhang X, et al. Development and future of vertical cavity surface emitting lasers operated at high temperatures(invited) [J]. Acta Photonica Sinica, 2022, 51(2):

0251201.

[10] Gehrsitz S, Reinhart F K, Gourgon C, et al. The refractive index of $Al_xGa_{1-x}As$ below the band gap: accurate determination and empirical modeling[J]. Journal of Applied Physics, 2000, 87 (11): 7825-7837.

[11] Blakemore J S. Semiconducting and other major properties of gallium arsenide[J]. Journal of Applied Physics, 1982, 53(10): R123-R181.

[12] Choquette K D, Geib K M, Ashby C I H, et al. Advances in selective wet oxidation of AlGaAs alloys[J]. IEEE Journal of Selected Topics in Quantum Electronics, 1997, 3(3): 916-926.

[13] Babic D I, Corzine S W. Analytic expressions for the reflection delay, penetration depth, and absorptance of quarter-wave dielectric mirrors[J]. IEEE Journal of Quantum Electronics, 1992, 28(2): 514-524.

Study on Temperature Characteristics of DBR Based on Resonant Cavity Light Emitting Diode

Ren Kaibing, Li Jianjun*, Cui Yuzheng, Zhang Zhendong, Fu Congle, Deng Jun

Key Laboratory of Opto-Electronic Technology, Ministry of Education, Beijing University of Technology, Beijing 100124, *China*

Abstract

Objective Resonant cavity light emitting diode (RCLED) has wide applications in fields such as display lighting and optical fiber communication due to its superior features and lower cost compared with ordinary light emitting diodes (LEDs) and vertical-cavity surface-emitting laser (VCSEL). RCLED with an outgoing wavelength of 650 nm needs to be coupled with optical fiber for plastic fiber communication, the coupling efficiency is related to the far-field distribution of outgoing light of RCLED. In addition, the temperature change will affect the far-field distribution of outgoing light of RCLED. As an important component of RCLED, distributed Bragg reflectors (DBRs) have an important influence on the performance of RCLED devices. Therefore, it is of great significance to study the influence of temperature on DBR characteristics. In this paper, the DBR structure is designed and prepared based on RCLED of 650 nm. The effect of temperature change on the reflection spectrum of DBR is simulated, and the white light reflection spectrum of DBR is tested by the test equipment to verify the correctness of the simulation results.

Methods In order to study the effect of temperature on DBR characteristics, the conclusion is drawn through theoretical simulation, and the experiments are used to verify the conclusion. First of all, the DBR structure based on RCLED of 650 nm is designed, and the material based on DBR must have the characteristic of a high and low refractive index material. In terms of material selection, by considering the absorption of red light and the oxidation of materials, the high and low refractive index materials are selected as $Al_{0.5}Ga_{0.5}As$ and $Al_{0.95}Ga_{0.05}As$ respectively. After determining the constituent material of the DBR, through the fitting function of the refractive index of $Al_xGa_{1-x}As$ material given in "the refractive index of $Al_xGa_{1-x}As$ below the band gap: accurate determination and empirical modeling", the relationship between the refractive index of $Al_xGa_{1-x}As$ and the incident wavelength, temperature, and the component of Al is obtained. Then we further determine the refractive index of $Al_{0.5}Ga_{0.5}As$ and $Al_{0.95}Ga_{0.05}As$ at room temperature at 650 nm and select the constituent log of DBR as 30 pairs. Later, the reflection spectrum of the DBR composed of 30 pairs of $Al_{0.5}Ga_{0.5}As$ and $Al_{0.95}Ga_{0.05}As$ at different temperatures is simulated, and the temperature characteristics of the theoretically simulated DBR are obtained. Finally, the designed DBR structure is prepared by the metal-organic chemical vapor deposition (MOCVD) experiment and tested, and the temperature characteristics of the experimental DBR are obtained and compared with the theoretically simulated results.

Results and Discussions Firstly, for the RCLED of 650 nm-based DBR design, in terms of the selection of materials constituting DBR, based on the relationship between the band width of $Al_xGa_{1-x}As$ material and Al (Fig. 1), the material with higher refractive index is determined to be $Al_{0.5}Ga_{0.5}As$, and as the component of Al gets higher, the device oxidation is more likely to happen. The material with a lower refractive index is determined as $Al_{0.95}Ga_{0.05}As$. Then, by the fitting function of the refractive index of $Al_xGa_{1-x}As$ and the three variables, namely the component of Al, temperature, and incident wavelength (Eq. 3), the relationship between the refractive index of $Al_xGa_{1-x}As$ and these three variables is obtained (Fig. 2) at 293.15 K with the incident wavelength of 650 nm. The refractive indices of $Al_{0.5}Ga_{0.5}As$ and $Al_{0.95}Ga_{0.05}As$ are 3.4386 and 3.1215, respectively; the thickness of $Al_{0.5}Ga_{0.5}As$ and $Al_{0.95}Ga_{0.05}As$ is determined as 47.258 nm and 52.059 nm, respectively in room temperature. Later, the pairs of DBR are determined as 30 by the relationship between the reflectivity and pairs of the DBR in different material combinations (Fig. 3). Then, according to the theory of thin film transmission matrix, the reflection spectrum of the DBR at different temperatures is simulated (Fig. 4), and it is found that the reflection spectrum of DBR moves towards the long wavelength and then through the central reflection wavelength of DBR at different temperatures (Fig. 5). The temperature drift rate of the central reflection wavelength of DBR is 0.048982 nm/℃. Finally, the designed DBR is prepared through the MOCVD experiment, and the white light reflection spectra at different temperatures are tested (Fig. 6). The redshift of DBR with the temperature is obtained. According to the relationship between the central reflection wavelength of DBR and temperature (Fig. 7), the drift rate of the center wavelength with temperature is 0.049277 nm /℃.

Conclusions For the far-field distribution of RCLED, the DBR structure based on RCLED of 650 nm is designed, and then the effect of temperature on DBR characteristics is analyzed. Temperature changes the optical thickness of each layer of the DBR by affecting the refractive index of the material $\mathrm{Al}_x\mathrm{Ga}_{1-x}\mathrm{As}$ of the DBR, thus affecting the reflection spectrum of the DBR. According to the theoretically simulated results, the reflection spectrum of DBR appears redshifted to the long wavelength as the temperature increases, and the temperature drift rate of the reflected wavelength of the DBR is calculated by linear fitting. From the experimental test results, as the temperature increases, the white light reflection spectrum of the prepared DBR also appears redshift phenomenon, and the temperature drift rate of the DBR central reflection wavelength calculated by linear fitting is not much different from the theoretically simulated results, which verifies the theoretical simulation. The analysis of the temperature characteristics of DBR makes the device designed at high temperature realize the wavelength matching between quantum trap and DBR, the conclusion has certain guiding significance for designing VCSEL devices with higher temperature sensitivity.

Key words resonant cavity light emitting diode; distributed Bragg reflector; temperature; dispersion relation; epitaxy